Superconductor Science and Technology

PAPER

Enhancement of critical current density in $CaKFe_4As_4$ single crystals through 3 MeV proton irradiation

To cite this article: N Haberkorn *et al* 2020 *Supercond. Sci. Technol.* **33** 025008

IOP Publishing Superconductor Science and Technology
Supercond. Sci. Technol. **33** (2020) 025008 (9pp) https://doi.org/10.1088/1361-6668/ab5f4b

Enhancement of critical current density in $CaKFe_4As_4$ single crystals through 3 MeV proton irradiation

N Haberkorn[1,2], M Xu[1,3], W R Meier[1,3], S Suárez[2], S L Bud'ko[1,3] and P C Canfield[1,3]

[1] Ames Laboratory, US DOE, Iowa State University, Ames, Iowa 50011, United States of America
[2] Centro Atómico Bariloche and Instituto Balseiro, CNEA and Consejo de Investigaciones Científicas y Técnicas Av. E. Bustillo 9500, R8402AGP, S. C. Bariloche, RN, Argentina
[3] Department of Physics and Astronomy, Iowa State University, Ames, Iowa 50011, United States of America

E-mail: nhaberk@cab.cnea.gov.ar

Received 6 September 2019, revised 27 November 2019
Accepted for publication 5 December 2019
Published 7 January 2020

Abstract

We study the influence of random point disorder on the vortex dynamics and critical current densities J_c of $CaKFe_4As_4$ single crystals by performing magnetization measurements. Different samples were irradiated with a proton (p) beam at constant energy of 3 MeV to fluencies from 2×10^{15} p cm^{-2} to 4×10^{16} p cm^{-2}. The results show the addition of extrinsic random point disorder enhances the J_c values at low and intermediate temperatures over the entire range of magnetic fields applied. The optimum pinning enhancement is achieved with a proton fluence of 3×10^{16} p cm^{-2}, increasing J_c at 5 K by factors ≈5 and 14 at self-field and $\mu_0 H = 3$ T, respectively. We analyze the vortex dynamics using the collective creep theory. The enhancement in J_c matches with a systematic reduction in the flux creep relaxation rates as a consequence of a gradual increase in the collective pinning energy U_0. The substantial increment in J_c produced by random point disorder, reaching values of 9 MA cm^{-2} at 5 K and self-field, makes $CaKFe_4As_4$ a promising material for applications based on current carrying capacity at high magnetic fields.

Keywords: iron based superconductors, critical current densities, irradiation

(Some figures may appear in colour only in the online journal)

1. Introduction

The current carrying capacity in superconducting materials depends on the intrinsic superconductor parameters and flux pinning. Technological applications such as superconductor magnets usually require an adequate operation temperature (related to the critical temperature, T_c), large upper critical fields H_{c2}, and small upper critical field anisotropy γ [1]. Flux pinning refers to the ability to trap vortices on crystalline defects. The latter can be intrinsic to the material such as vacancies and twin boundaries, or added extrinsically such as random disorder and precipitates [1, 2]. The discovery of iron-based superconductors (IBS) allows for an expansion of the knowledge on the interplay between intrinsic thermal fluctuations and vortex pinning [2–5]. Moreover, the span of different properties makes them attractive for applications. The recently discovered $CaKFe_4As_4$ displays unusual features in the vortex pinning as a consequence of a particular defect structure [6, 7]. $CaKFe_4As_4$ crystallizes in a tetragonal structure. It has $T_c = 35$ K, an extrapolated H_{c2} (0) > 70 T with the in-plane coherence length ${}^{ab}_{GL}(0) \approx 1.4$ nm and the penetration depth ${}^{ab}(0) = 208$ (4) nm [8, 9]. The anisotropy parameter $\gamma = H_{c2}^{//ab} / H_{c2}^{//c}$ reduces with the temperature being ≈1.5 at 25 K and 2.5 near T_c [9]. Despite being a superconductor with small γ, the magnetic field dependence **H** of the critical current density J_c exhibits high anisotropy.

Indeed, $J_c^{H\|ab}$ is up to one order of magnitude higher than $J_c^{H\|c}$ [7, 10, 11]. Moreover, $J_c^{H\|c}$ displays an unusual peak in temperature [10–12]. The sources of pinning in $CaKFe_4As_4$ single crystals are stacking faults [11], planar $CaFe_2As_2$ intergrowth [7], random point disorder [13], and regions in which the superconducting order parameter suppress (size comparable to the coherence length, ξ) [14]. The strong vortex pinning for $\mathbf{H}||ab$ originates in the planar defects [7, 11]. However, for $\mathbf{H}||c$, the vortex pinning at low temperatures is mostly weak. The latter is evident in large vortex creep rates and the small critical current-density ratio $J_c/J_0 \approx 1.4\%$ (with $J_0 = cH_c/3\sqrt{6}\pi\lambda$ the depairing critical current, c the speed of light, and H_c the thermodynamic critical field) [13]. The peak in the $J_c^{H\|c}$ (T) appears as a consequence of the emergence of new pinning centers in a regime dominated mainly by random point disorder [15]. The low pinning in pristine crystals agrees with the fact that substitutional disorder produced by Ni-substitution masks the peak in $J_c^{H\|c}$ (T) [13].

It is usually accepted that the best way to improve pinning in superconductor materials is by combining different types of pinning centers [1]. These include second phases (nanorods or nanoparticles), point defects, and structural disorder such as twin boundaries and stacking faults [16–19]. The particular microstructure of $CaKFe_4As_4$ with stacking faults and $CaFe_2As_2$ intergrowths makes it promising for the analysis of the influence of mixed pinning landscapes on its resulting J_c values. The standard method to introduce defects in a controlled way is particle irradiation. For any superconductor, the maximum electrical current density is determined by the vortex pinning defects that can be tailored into the material without degrading the superconductor properties. Depending on the mass and energy of the ions and the properties of the superconducting material, irradiation allows for the production of defects such as points, clusters, or tracks [1]. Whereas the pinning produced by random disorder and clusters is isotropic, pinning produced by tracks can be highly anisotropic. The effectiveness of random point disorder enhancing J_c has been verified in different IBS such as FeSe [20], Co-doped $BaFe_2As_2$ [21, 22] and $Ba_{1-x}K_xFe_2As_2$ [23], among others. On the other hand, the vortex pinning in these materials is also largely improved by amorphous tracks [24–27].

Here, we show the influence of add random point disorder on the pinning and vortex dynamics of $CaKFe_4As_4$ single crystals. Different samples where irradiated with 3 MeV protons to fluencies up to 4×10^{16} p cm^{-2}. The J_c values at low and intermediate temperatures increase in the entire range of magnetic fields. For instance, at the optimal fluence of 3×10^{16} p cm^{-2}, J_c at 5 K increases by factors ≈5 and 14 at self-field and $\mu_0 H = 3$ T, respectively. The significant and systematic enhancement in the J_c values at low and intermediate temperatures correlates with a substantial reduction in the flux creep relaxation rates. The analysis of the vortex dynamics in the framework of the collective creep theory indicates that irradiation produces gradual increment in the pinning energy U_0.

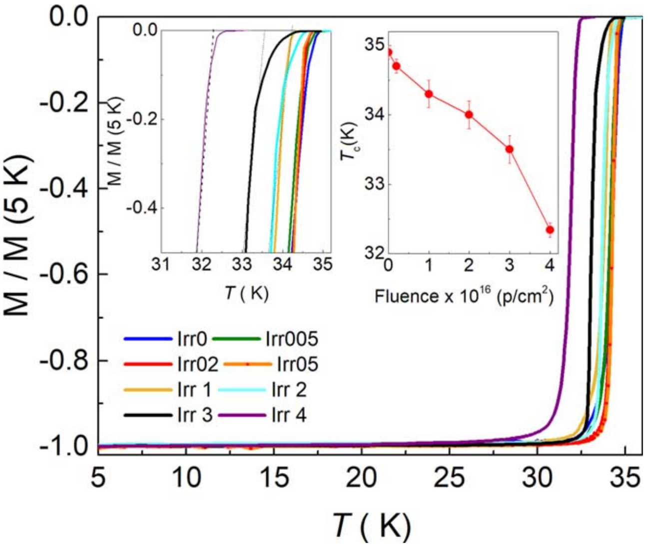

Figure 1. Normalized magnetization versus temperature for $CaKFe_4As_4$ single crystals irradiated with different proton doses. The data corresponds to $\mu_0 H = 1$ mT applied parallel to the c-axis. Inset at the right shows the T_c as function of the proton fluence. Inset at the left shows the criterion used to determine T_c applied to the Irr3 sample.

2. Material and methods

Single crystals of $CaKFe_4As_4$ were grown using the procedure described in [9] and [28]. We use plate-like single crystals with length l, width, w, and thickness d around 0.15 cm, 0.1 cm and 0.002–0.003 cm, respectively. Magnetization measurements were collected using a Quantum Design SQUID magnetometer. The thicknesses d were calculated from Meissner slopes with $\mathbf{H}||ab$ using the area $(l \times w)$ and the superconductor volume [13]. We extracted $J_c(T)$ from the magnetization data using the Bean Model [29, 30]. For $\mathbf{H}||c$, $J_c = \frac{20\Delta M}{w(1 - w/(3l))}$, where ΔM is the difference in magnetization between the top and bottom branches of the hysteresis loop. The flux creep rate, $S = -\delta \ln J/\ln t$ was recorded as a function of time, t, over periods of 1 h using a scan length of 3 cm. The magnetization of the sample holder was measured and subtracted from the data by averaging the initial points of the time relaxation for the lower and upper magnetic branches.

The single crystals were irradiated with 3 MeV protons along the normal of the crystal plane (parallel to the c-axis) using a 1.7 MV tandem accelerator. Typical beam currents of ≈30 nA were used. The crystals were fixed to the holder with silver paint. The irradiations were performed with the ion beam positioned at the center of the sample (size spot ≈1.8 mm). The 3 MeV protons produce mainly random point defects and also some nanoclusters of a few nanometers in size [17, 31]. Simulations using the SRIM-TRIM software package [32] indicate that irradiation with 3 MeV protons produces a damage profile in which most of the ion's cross the samples. The so-called Bragg peak (energy loss of ionizing radiation during its travel through matter) for $CaKFe_4As_4$ is at around 40 μm, being a distance larger than the thickness of the single

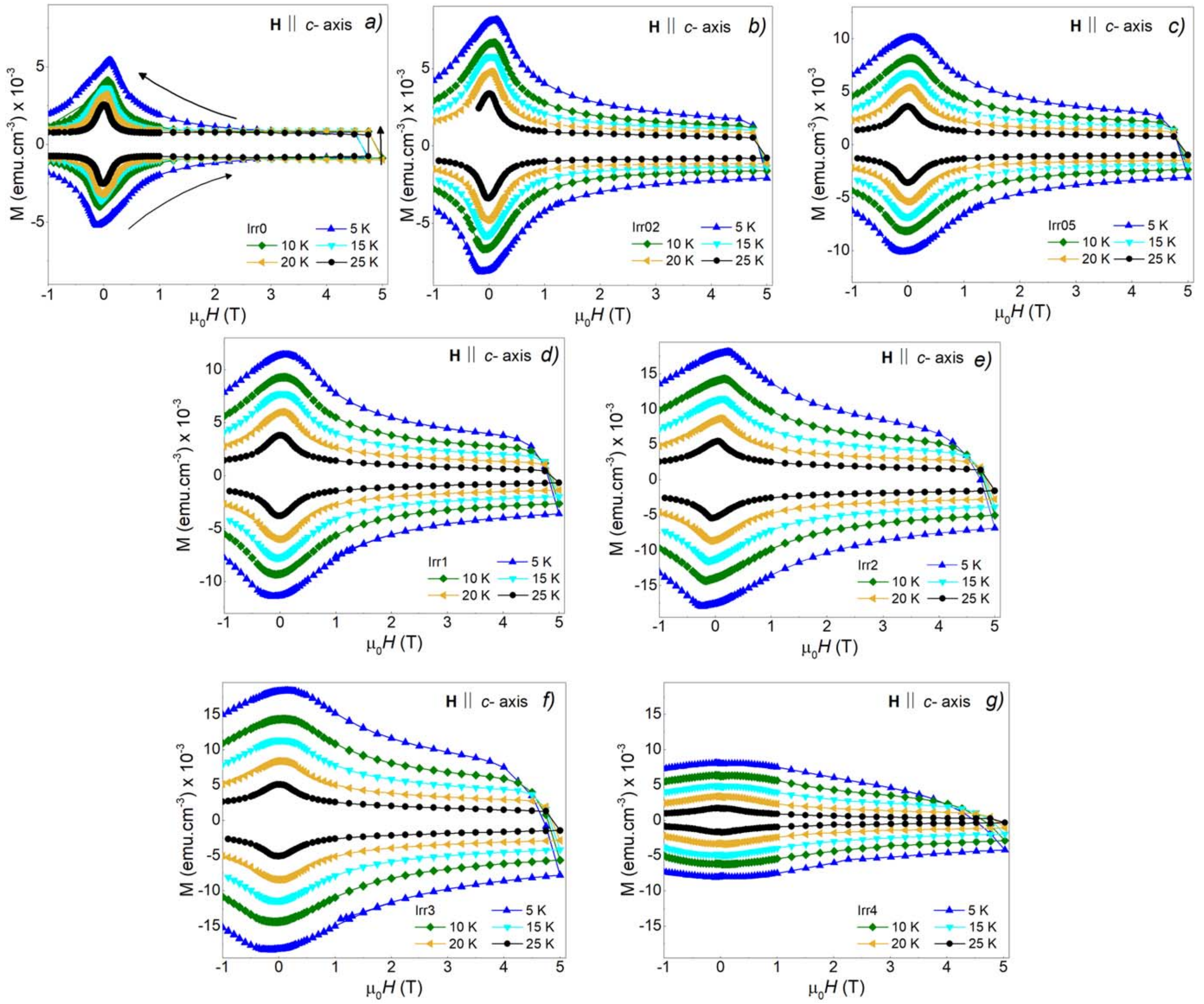

Figure 2. (a)–(g) Magnetization loops under $\mathbf{H}||c$ for pristine and irradiated CaKFe$_4$As$_4$ crystals. The curves correspond to magnetic fields between $\mu_0 H = -1$ T and 5 T. Data for pristine crystal in panel (a) are taken from the [13].

crystals used ($\leqslant 30\,\mu$m). Wherever used, the notation Irrx indicates a CaKFe$_4$As$_4$ single crystal without irradiation ($x = 0$), and $x = 02$ ($2 \times 10^{15}\,\mathrm{p\,cm^{-2}}$), 05 ($5 \times 10^{15}\,\mathrm{p\,cm^{-2}}$), 1 ($1 \times 10^{16}\,\mathrm{p\,cm^{-2}}$), 2 ($2 \times 10^{16}\,\mathrm{p\,cm^{-2}}$), 3 ($3 \times 10^{16}\,\mathrm{p\,cm^{-2}}$) and 4 ($4 \times 10^{16}\,\mathrm{p\,cm^{-2}}$).

3. Results and discussion

Figure 1 shows the temperature dependence of the normalized magnetization (M (T)/M (5 K)) for the studied single crystals. The measurements were performed with $\mathbf{H}||c$ under zero-field cooling with an applied magnetic field of 1 mT. The criterion for T_c determination, maximum slope of M (T) data extrapolated up to the M (T)/M (5 K) = 0 line, is shown in left inset in figure 1. The tails at the onsets and offsets of the curves may be related with non-uniform irradiation at the corners. The $T_c = 34.8$ K for pristine crystal is gradually suppressed as irradiation fluence increases. For Irr4 (the maximum fluence), T_c reduces to $\approx$32.4 K (see right inset in figure 1). The suppression of T_c with random disorder in CaKFe$_4$As$_4$ was previously discussed in [33]. The changes in T_c and the variations λ (T) at low-temperatures agree with a multi-band superconductor with $s\pm$ pairing [34].

Figure 2 shows hysteresis loops for the pristine and irradiated crystals under $\mathbf{H}||c$ at several temperatures. The loops are almost symmetric with respect to both H- and M-axes, indicating that bulk pinning dominates. The evolution of the J_c under magnetic field as a function of the irradiation fluence for temperatures between 5 and 25 K is summarized in figures 3(a)–(e). The results show that J_c (H) values enhance systematically as irradiation fluence increases up to $3 \times 10^{16}\,\mathrm{p\,cm^{-2}}$ and decrease for Irr4. Upon irradiation to a dose of $3 \times 10^{16}\,\mathrm{p\,cm^{-2}}$, J_c systematically enhances at low and intermediate temperatures across the whole range of fields. An exception is observed at $T \geqslant 20$ K for Irr1, which may be related to differences in J_c (H) at high magnetic fields and temperatures in the pristine samples (usually related to a

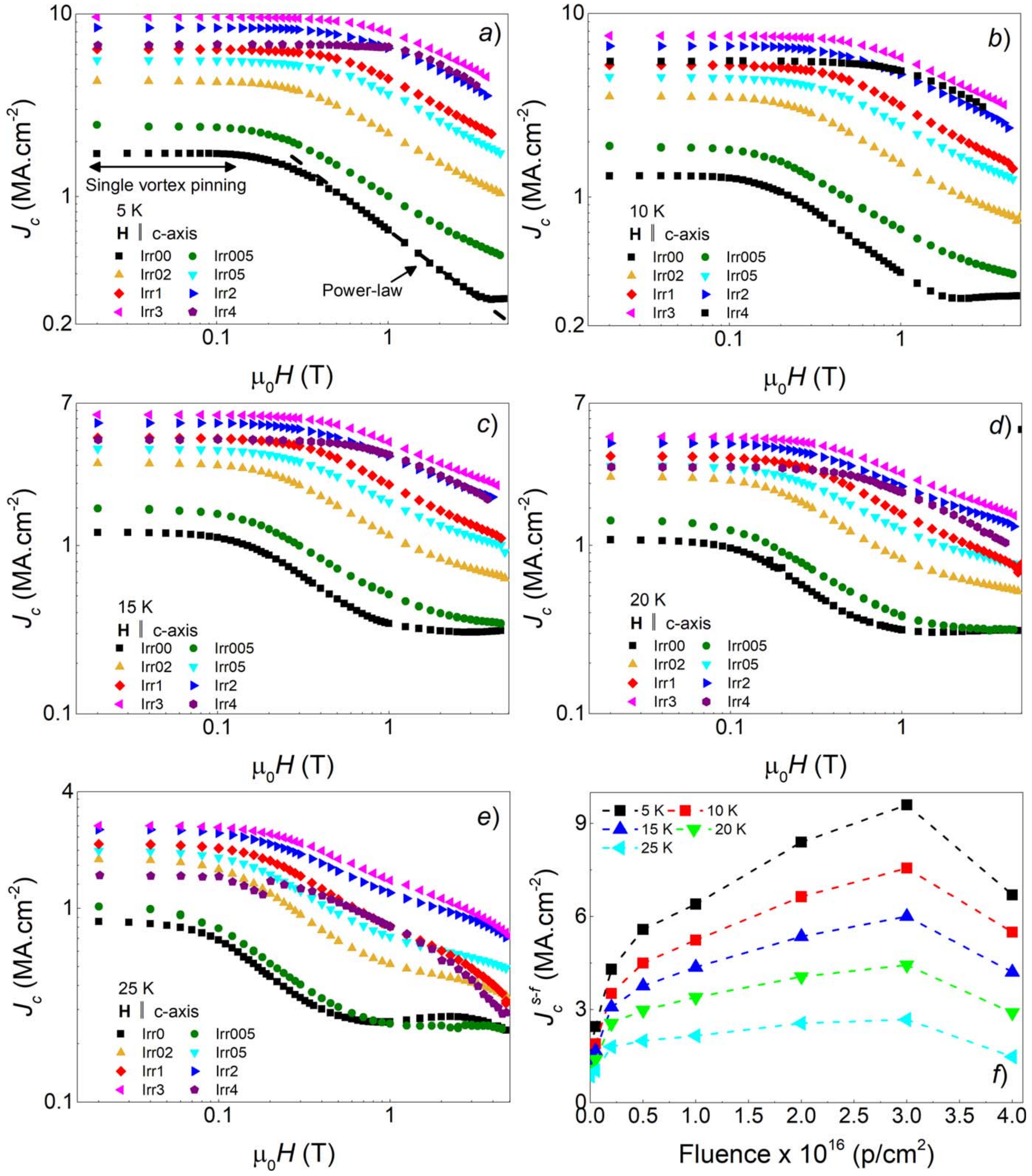

Figure 3. (a)–(e) Magnetic field dependence of the critical current densities J_c in for CaKFe$_4$As$_4$ single crystals irradiated with different proton fluencies at 5 K, 10 K, 15 K, 20 K and 25 K, respectively. (f) Summary of the self-field critical current densities J_c^{sf} as function of the proton fluence for several temperatures. Criterion for α determination is included in panel (a).

modulation in J_c (H) due to a second peak in the magnetization) [13]. The comparison of the self-field critical current J_c^{sf} as a function of irradiation fluence is shown in figure 3(f). As we mention above, J_c^{sf} values enhance systematically as irradiation fluence increases up to 3×10^{16} p cm^{-2} and decreases for Irr4. For instance, at 5 K the J_c^{sf} value rises from $\approx$1.7 MA cm^{-2} for Irr0 to $\approx$ 9 MA cm^{-2} for Irr3. In addition to the substantial enhancement of J_c at low magnetic fields, the J_c (H) dependences improve with the irradiation for higher fields. The pristine single-crystal displays different regimes

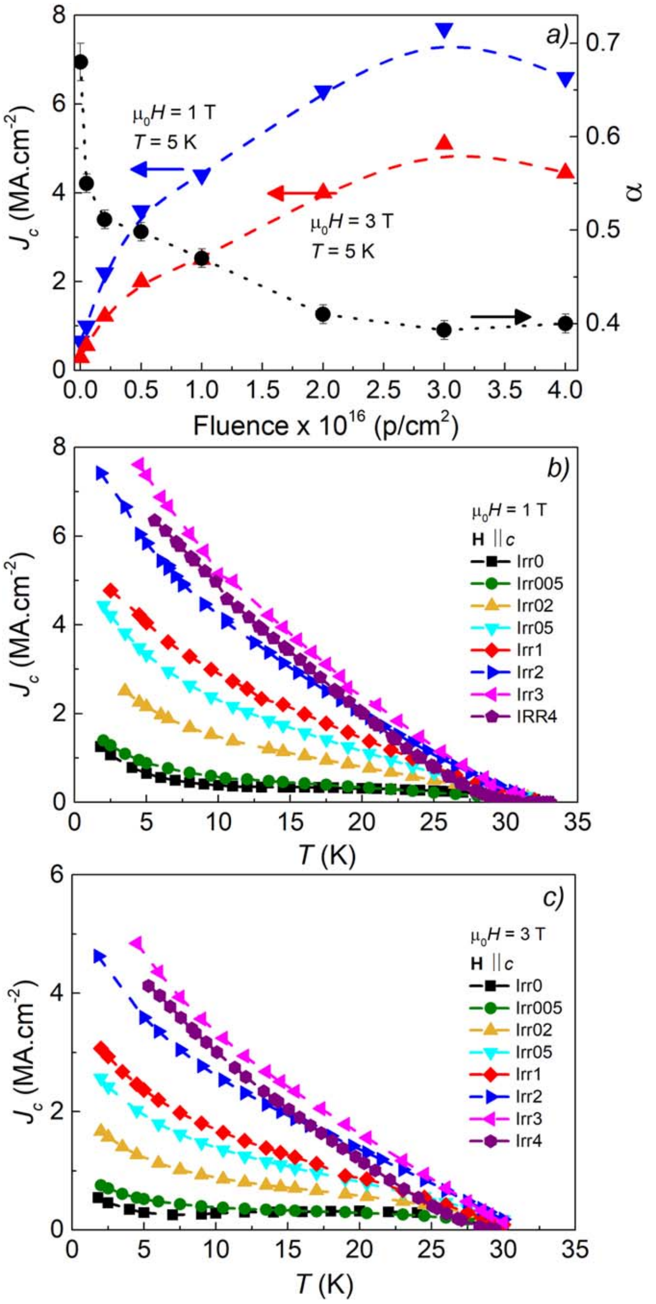

Figure 4. (a) Dependence of the critical current density J_c for $\mu_0 H = 1$ T and 3 T at 5 K (left axis) and α exponent (right axis) with the proton fluence for CaKFe$_4$As$_4$ single crystals. (b), (c) Temperature dependence of the critical current densities J_c for the different studied single crystals with $\mu_0 H = 1$ T and $\mu_0 H = 3$ T, respectively.

previously discussed in [13]: (I) at low field $J_c \approx$ constant that could be associated to single vortex pinning; (II) a power-law dependence $J_c \propto H^{-\alpha}$ related to strong pinning centers; (III) a third regime (at the end of the power-law) related to random disorder with J_c $(H) \approx$ constant or a modulation with a peak originated from the second peak in the magnetization (SPM); and (IV) a high-field regime which is characterized by a fast drop in $J_c(H)$ and is usually related to a crossover from elastic to plastic relaxation of the vortex lattice [34]. The regime (I) extends to higher fields for Irr4 than for the other samples (see figure 3(a)). This fact can be related to the influence of the thickness and the self-field in the J_c values at low fields [35]. Indeed, Irr4 has a thickness of 30 μm instead of the 20 μm for the rest of the single crystals, which reduces J_c at the regime (I) without affecting their values at regime (II). Considering that the J_c values at the regime (II) for Irr4 are smaller than for Irr3, the resulting J_c^{sf} should be smaller in Irr4 than in Irr3 when corrected for equal thickness [35].

The irradiation reduces the α exponent and masks the modulation in J_c (H) at low temperatures. Features related to a SPM remain at intermediate and high temperatures, even for high irradiation fluencies. Figure 4(a) (right y-axis) shows the evolution of the α exponent with irradiation fluence for J_c (H) at 5 K. Similar α exponents than for 5 K are observed up to 25 K, indicating that the vortex pinning at the power-law regime is provided by mixing of extrinsic random disorder and other defects present in the pristine crystals. The thermal fluctuations manifest as a shift to lower fields in the vortex crossovers between the different regimes. The result shows a fast decrease in α from $\approx$0.68 in the pristine crystal to $\approx$0.51 for Irr02, which is in agreement with a low defect density in the former [13]. As irradiation fluence increases α reduces, reaching a value of $\approx$0.4 for Irr3 and Irr4. A similar evolution of α reaching a minimum value of approximately 0.4, has been previously observed in cuprate thin films [17]. The value of α depends on the pinning landscape and usually decreases with a mixing of random disorder with other sources of pinning. Typical values ranges from $\approx$0.5 to 0.6 for nanoparticles [36] to $\approx$0.2 for mixed pinning landscapes with correlated disorder [37]. Intermediate values are typically observed in mixed pinning landscapes including strong and weak pinning centers [17, 22].

For CaKFe$_4$As$_4$, the introduction of small random defects via irradiation and the change in α improve significantly the in-field dependences of J_c at low and intermediate temperatures. For instance, at 5 K for $\mu_0 H = 1$ T and $\mu_0 H = 3$ T, the J_c values in Irr3 increases in factors $\approx$9.5 and 14 with respect to the pristine crystal. It is important to note that the $J_c^{H\|c}$ (T) peak usually observed in pristine crystals [7, 10–12] is masked for irradiation fluencies higher than 2×10^{15} p cm^{-2}. Moreover, the enhancement of J_c at high magnetic fields takes place at $T < 25$ K, where random disorder produces more effective vortex pinning (see figures 4(b) and (c)) [17]. In addition to the low effectiveness of small pinning centers to trap vortices close T_c, the J_c values at high temperatures in the irradiated crystals may also be affected by an increment in the vortex fluctuations due to variations in the superfluid density as a consequence of high disorder at the nanoscale [38].

To analyze in detail the correlation between the enhancement in J_c and the resulting vortex dynamics, we performed magnetic relaxation measurements of the persistent currents for proton fluencies up to 3×10^{16} p cm^{-2}. The collective creep theory predicts a temperature dependence of the normalized flux creep rates as:

$$S = -\frac{d(\ln J)}{d(\ln t)} = \frac{T}{U_0 + \mu T\,\ln(t/t_0)} = \frac{T}{U_0}\left(\frac{J}{J_c}\right)^{\mu}, \qquad (1)$$

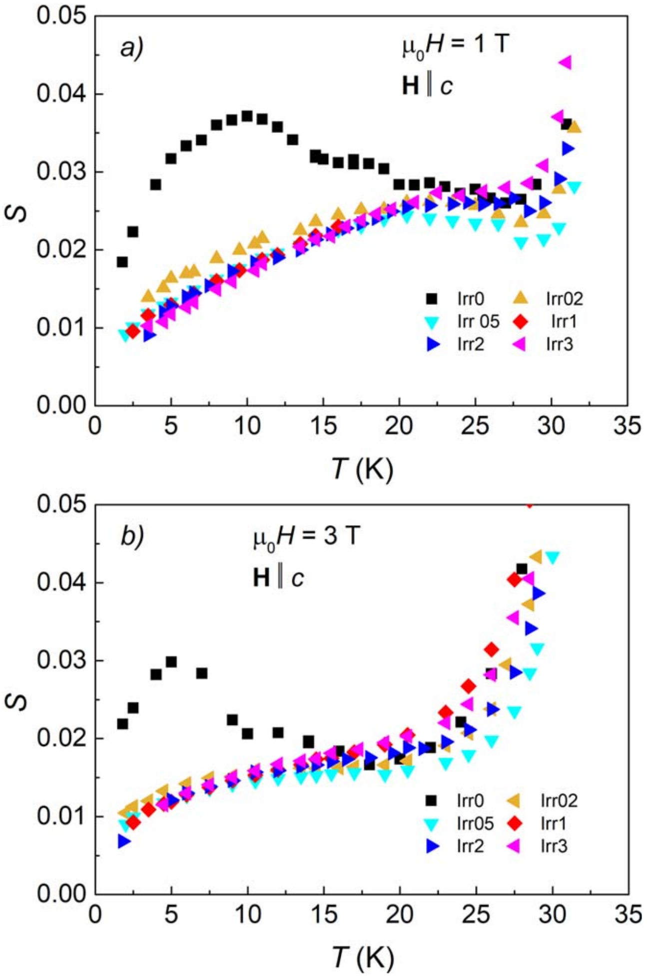

Figure 5. (a), (b) Temperature dependence of the flux creep rates S for $CaKFe_4As_4$ single crystals irradiated with different proton fluencies for $\mu_0H = 1$ T and $\mu_0H = 3$ T, respectively.

where t_0 is a vortex hopping attempt time, U_0 is the collective pinning barrier at $T = 0$ in the absence of a driving force, and $\mu > 0$ is the regime-dependent glassy exponent determined by the bundle size and vortex lattice elasticity [39]. Based on the model of nucleation of vortex loops, for random point defects in the three-dimensional case, μ is $1/7$, $3/2$–$5/2$, and $7/9$ for single vortex regime (SVR), small-bundle, and large-bundle creep, respectively. It is important to note that, despite specific numbers for the bundle size theoretically predicted [39], the experimental μ values usually evolve gradually with magnetic fields [40]. As we have shown in [13], pristine $CaKFe_4As_4$ crystals display high S values even for low temperatures, which is a signature of low U_0 values. A distinctive feature in its vortex dynamics is a systematic increment in U_0 with temperature due to the emergence of new pinning centers [7, 11, 12]. Figures 5(a) and (b) show S (T) dependences for $\mu_0H = 1$ T and $\mu_0H = 3$ T, respectively. The results show that in comparison with the pristine crystals, the damage produced by the irradiation provides a substantial reduction in the S values at low and intermediate temperatures. On the other hand, for irradiated samples, minimal changes are observed at low temperatures, and slight variations occur at high temperatures. The small shifts in the crossover to faster creep near T_c indicate that random disorder slightly modifies the temperature in which the crossover from elastic to plastic motion takes place [35].

To analyze in more detail the influence of random disorder on vortex dynamics, we extract U_0 and the μ exponent that determines the S values at intermediate temperatures using the Maley analysis [41]. According to vortex-glass and collective creep theories [39], the effective activation energy as a function of current density (J) is given by

$$U_{eff} = \frac{U_0}{\mu}\left[\left(\frac{J_c}{J}\right)^{\mu} - 1\right]. \tag{2}$$

The Maley method considers that the current density decays as $\frac{dJ}{dt} = -\left(\frac{J_c}{\tau}\right)e^{-\frac{U_{eff}(J)}{T}}$, and the effective activation energy $U_{eff}(J)$ is described by $U_{eff} = -T\left[\ln\left|\frac{dJ}{dt}\right| - C\right]$ (with C, a constant factor). The analysis requires the consideration of a thermal factor $G(T)$, which results in $U_{eff}(J, 0) \approx U_{eff}(J, T)/G(T)$ [42]. Figures 6(a) and (b) show the Maley analysis and the corresponding fits using equation (2) for the different samples with $\mu_0H = 1$ T and $\mu_0H = 3$ T, respectively. Insets show the respective G (T) dependences to maintain the 'piecewise' continuity. The data for Irr0 are not included due to changes in U_0 with temperature [13]. It is important to note that the analysis considers that the vortex mechanism is not affected by temperature. Therefore, the fits were performed at T typically smaller than 15 K, which corresponds to the temperature range where the data for $\mu_0H = 1$ T and $\mu_0H = 3$ T have the power-law behavior (see figures 3(a)–(e)). Figures 6(c) and (d) show the exponent μ and the U_0 values for the different irradiation fluencies. The results show μ exponents in a range between 1.4 and 2, which in collective creep theory are within the expectations for small bundles. The values are systematically higher for $\mu_0H = 3$ T than $\mu_0H = 1$ T. Moreover, as irradiation fluence increases, μ reduces. A similar behavior is observed in cuprates [43] and has been related to the influence of random point disorder in mixed pinning landscapes [44]. On the other hand, the irradiation produces a significant increment in U_0. The initial values of a few tens of K (evidenced from the high S values at low temperatures) in the pristine crystal systematically increase with the irradiation fluence, reaching ≈200 K for Irr3. Inset figures 6(c) and (d) show the S (T) dependences for Irr05 and Irr3 and the corresponding data using equation (1) with the obtained U_0 and μ, and $\ln(t/t_0) = 26$ [45]. A good correlation between the data is obtained.

The results show that the addition of random point disorder and nanoclusters enhances J_c at low and intermediated temperatures. The optimum pinning enhancement is achieved with a dose of 3×10^{16} p cm^{-2}. The changes in J_c (H, T) show a clear correlation with an increment in U_0. We found that for the optimum dose, J_c at 5 K increases by factors ≈5

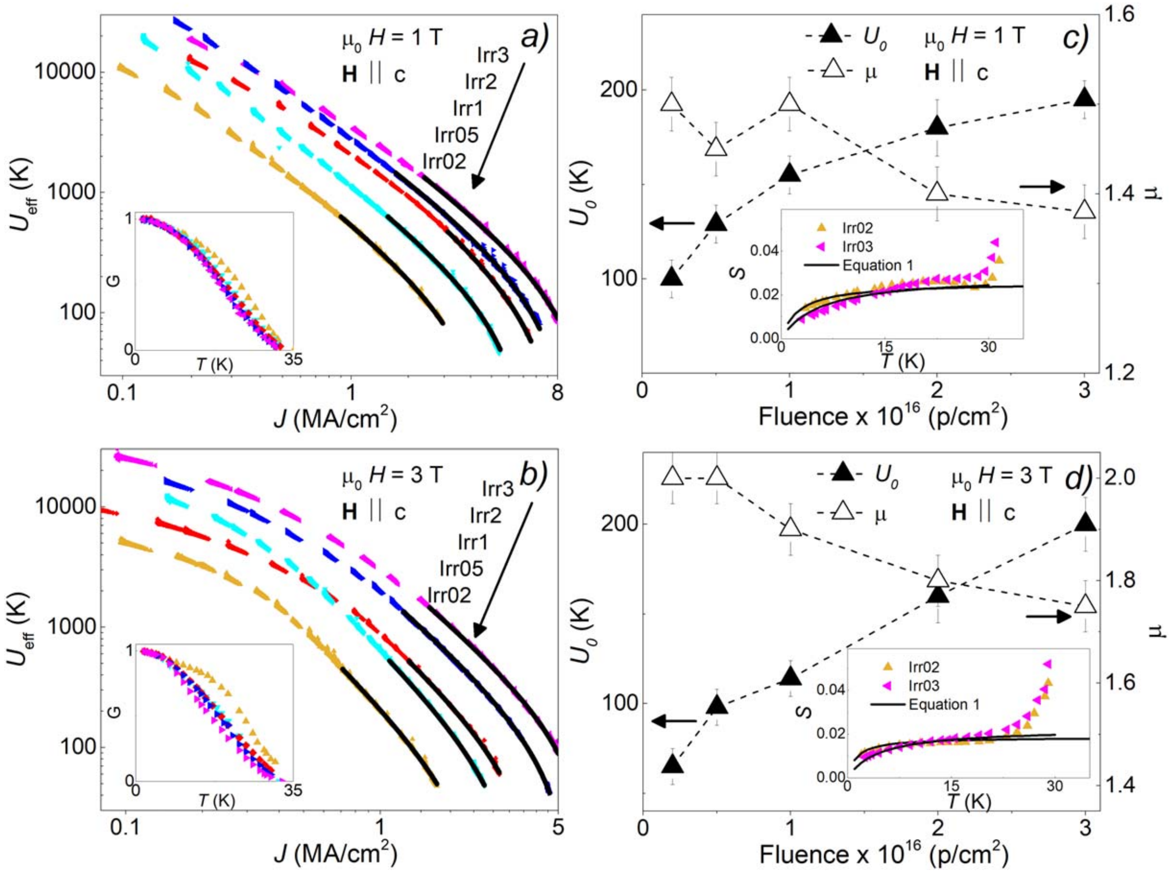

Figure 6. (a), (b) Maley analysis with $\mu_0 H = 1$ T and $\mu_0 H = 3$ T, respectively. Insets show the corresponding G(T) functions used to maintain the piecewise continuity. (c), (d) U_0 (left y-axis) and μ (right y-axis) for $\mu_0 H = 1$ T and $\mu_0 H = 3$ T, respectively. Insets shows S (T) functions for Irr02 and Irr3 using equation (1) with $\ln(t/t_0) = 26$ and the respective data.

and ≈14 at self-field and $\mu_0 H = 3$ T, respectively. The obtained values are close to those observed in proton irradiated $Ba_{0.6}K_{0.4}Fe_2As_2$ with $T_c \approx 38.6$ K where a maximum J_c value of ≈ 11 MA cm^{-2} at 2 K for a fluence of 5.8×10^{16} p cm^{-2} [23]. Furthermore, the enhancement in J_c is higher than that observed in proton irradiated Co-doped $BaFe_2As_2$ of ~2.6 [21, 22]. The differences may be related to the ξ values, which make the pinning produced by small defects more effective [9, 46–48]. The $J_c^{sf} \approx 9$ MA cm^{-2} for Irr3 corresponds to $(J_c/J_0) \approx (9/170) \approx 5\%$. Considering the SVR for random point disorder, the U_0 value can be estimated by $U_c \approx \frac{H_c^2 \xi^3}{\gamma}\left(\frac{J_c}{J_0}\right)^{\frac{1}{2}} \approx T_c\left(\frac{J_c\left(1-\left(\frac{T}{T_c}\right)\right)}{J_0 G_i}\right)^{\frac{1}{2}}$ (with G_i the Ginzburg number) [39]. An estimate for 5 K using ξ (0) = 1.4 nm [9], $\gamma \approx 1.2$ and $\lambda \approx 200$ nm [8], $G_i \approx 5.5 \times 10^{-4}$ and $J_c^{sf} \approx 9$ MA cm^{-2}, yields $U_0 \approx 300$ K. This value is in a good agreement with the data obtained at high magnetic fields. It is important to note the peak in $J_c^{H||c}$ (T) usually observed in pristine crystals disappears even for irradiation fluence of 2×10^{15} p cm^{-2}. This fact agrees with fundamentally weak pinning for $\mathbf{H}||c$ at low temperatures in the pristine $CaKFe_4As_4$ single crystals. The substantial enhancement in J_c produced by random point disorder for $\mathbf{H}||c$ and the strong pinning usually observed for $\mathbf{H}||ab$ make of the $CaKFe_4As_4$ system a potential material for applications based on current carrying capacity at high magnetic fields [4]. Moreover, like in $Ba_{0.6}K_{0.4}Fe_2As_2$, the in-field dependences of J_c for $\mathbf{H}||c$ might be significantly improved introducing correlated disorder [25, 26].

4. Conclusions

To summarize, we have studied the effect of proton irradiation for fluencies up to 4×10^{16} p cm^{-2} in $CaKFe_4As_4$ single crystals. The T_c systematically reduces from 34.8 K to 32.4 K as irradiation fluence increases. The addition of extrinsic random point disorder enhances the J_c values at low and intermediate temperatures in the entire range of magnetic fields. The optimum pinning enhancement is achieved with a proton fluence of 3×10^{16} p cm^{-2}, increasing J_c at 5 K by factors ≈5 and ≈14 at self-field and $\mu_0 H = 3$ T, respectively. Moreover, the peak in J_c (T) present in pristine crystals is completely masked, even for lower irradiation fluencies. For irradiated samples, the collective creep theory, with a unique μ and U_0 for every H, describe the flux creep relaxation rates. We found that the enhancement in J_c at low and intermediate temperatures matches with a regular increase in the collective pinning energy. The highest J_c values are reached for a fluence of $3 \times 10^{16}\,\mathrm{p\,cm^{-2}}$ and correspond to glassy exponents μ within expectations for small bundles and $U_0 \approx 200$ K. The substantial enhancement in J_c produced by random point disorder for $\mathbf{H}||c$ and the strong pinning usually observed for $\mathbf{H}||ab$ make $CaKFe_4As_4$ a promising material for applications based on current carrying capacity at high magnetic fields.

Acknowledgments

This work was supported by the US Department of Energy, Office of Basic Energy Science, Division of Materials Sciences and Engineering. The research was performed at the Ames Laboratory. Ames Laboratory is operated for the US Department of Energy by Iowa State University under Contract No. DE-AC02-07CH11358. WRM was supported by the Gordon and Betty Moore Foundation's EPiQS Initiative through Grant GBMF4411. NH and SS are partially supported by ANCYP PICT2015-2171 (Argentina).

ORCID iDs

N Haberkorn https://orcid.org/0000-0002-5261-1642
P C Canfield https://orcid.org/0000-0002-7715-0643

References

[1] Wai-Kwong K, Ulrich W, Andreas G, Koshelev Alexei E, Kihlstrom Karen J and Crabtree George W 2016 *Rep. Prog. Phys.* **79** 116501

[2] Eisterer M 2018 *Supercond. Sci. Technol.* **31** 013001

[3] Hosono H, Yamamoto A, Hiramatsu H and Ma Y 2018 *Mater. Today* **21** 278

[4] He H, Chao Y, Chiheng D, Xianping Z, Dongliang W, Zhe C, Jianqi L, Satoshi A, Haihu W and Yanwei M 2018 *Supercond. Sci. Technol.* **31** 015017

[5] Tamegai T, Sura T, Miyawaki D, Pyon S, Takano K, Kajitani H, Koizumi N and Awaji S 2019 *IEEE Trans. Appl. Supercond.* **29** 7300605

[6] Iyo A, Kawashima K, Kinjo T, Nishio T, Ishida S, Fujihisa H, Gotoh Y, Kihou K, Eisaki H and Yoshida Y 2016 *J. Am. Chem. Soc.* **138** 3410

[7] Shigeyuki I *et al* 2019 *NPJ Quantum Mater.* **4** 27

[8] Rustem K, Meier William R, Yun W, Daixiang M, Bud'ko S L, Ilya E, Hubertus L, Adam K, Canfield Paul C and Alex A 2018 *Phys. Rev.* B **97** 140503(R)

[9] Meier W R *et al* 2016 *Phys. Rev.* B **94** 064501

[10] Singh Shiv J, Matthew B, Meier William R, Patrick T, Blundell Stephen J, Canfield Paul C and Coldea Amalia I 2018 *Phys. Rev. Mater.* **2** 074802

[11] Sunseng P *et al* 2019 *Phys. Rev.* B **99** 104506

[12] Wang C, Hai L, Bing S and Hai-Hu W 2019 *Sci. Bull.* **64** 81

[13] Haberkorn N, Xu M, Meier W R, Schmidt J, Bud'ko S L and Canfield P C 2019 *Phys. Rev.* B **100** 064524

[14] Fente A, Meier W R, Kong T, Kogan V G, Bud'ko S L, Canfield P C, Isabel G and Hermann S 2018 *Phys. Rev.* B **97** 134501

[15] van der Beek C J *et al* 2010 *Phys. Rev.* B **81** 174517

[16] Kihlstrom J *et al* 2013 *Appl. Phys. Lett.* **103** 202601

[17] Jia Y *et al* 2013 *Appl. Phys. Lett.* **103** 122601

[18] Ji-Hwan K, Yifei M, Lijun W, Yimei Z, Yifei Z, Venkat S, Ulrich W, Wai-Kwong K and Jian-Min Z 2018 *Supercond. Sci. Technol.* **31** 105006

[19] Masashi M, Boris M, Takeharu K, Takashi S, Keisuke W, Seiji A and Keiichi T 2013 *Nat. Commun.* **4** 2499

[20] Yue S, Sunseng P, Tsuyoshi T, Ryo K, Tatsuya W, Shigeru K, Yuji M, Takasada S and Hisashi K 2015 *Appl. Phys. Exp.* **8** 113102

[21] Haberkorn N, Maiorov B, Usov I O, Weigand M, Hirata W, Miyasaka S, Tajima S, Chikumoto N, Tanabe K and Leonardo C 2012 *Phys. Rev.* B **85** 014522

[22] Toshihiro T, Yasuyuki N, Tsuyoshi T and Hisashi K 2012 *Phys. Rev.* B **86** 094527

[23] Toshihiro T, Fumiaki O, Sunseng P, Tsuyoshi T and Hisashi K 2015 *Supercond. Sci. Technol.* **28** 085003

[24] Yue S, Akiyoshi P, Sunseng P, Tsuyoshi T, Tadashi K and Ataru I 2017 *Phys. Rev.* B **95** 104514

[25] Ohtake F, Taen T, Pyon S, Tamegai T, Okayasu S, Kambara T and Kitamura H 2015 *Physica* C **518** 47

[26] Fang L *et al* 2012 *Appl. Phys. Lett.* **101** 012601

[27] Haberkorn N, Jeehoon K, Gofryk K, Ronning F, Sefat A S, Fang L, Welp U, Kwok W K and Civale L 2015 *Supercond. Sci. Technol.* **28** 055011

[28] Meier W R, Kong T, Bud'ko S L and Canfield P C 2017 *Phys. Rev. Mater.* **1** 013401

[29] Bean C P 1962 *Phys. Rev. Lett.* **8** 250
Bean C P 1964 *Rev. Mod. Phys.* **36** 31

[30] Gyorgy E M, Van Dover R B, Jackson K A, Schneemeyer L F and Waszczak J V 1989 *Appl. Phys. Lett.* **55** 283

[31] Civale L, Marwick A D, McElfresh M W, Worthington T K, Malozemoff A P, Holtzberg F H, Thompson J R and Kirk M A 1990 *Phys. Rev. Lett.* **65** 1164

[32] Ziegler J F, Biersack J P and Ziegler M D 2015 *SRIM, The Stopping and Range of Ions in Matter* 15th edn (Morrisville, NC, 27560 USA: Lulu Press Co.) http://srim.org/SRIM%20Book.htm

[33] Teknowijoyo S, Cho K, Kończykowski M, Timmons E I, Tanatar M A, Meier W R, Xu M, Bud'ko S L, Canfield P C and Prozorov R 2018 *Phys. Rev* B **97** 140508(R)

[34] Prozorov R *et al* 2008 *Phys. Rev.* B **78** 224506

[35] Alvaro S, Carles N, Nuria D-V, Du-Xing C and Clem John R 2010 *Appl. Phys. Lett.* **96** 072510

[36] van der Beek C J, Konczykowski M, Abal'oshev A, Abal'osheva I, Gierlowski P, Lewandowski S J, Indenbom M V and Barbanera S 2002 *Phys. Rev.* B **66** 024523

[37] Maiorov B, Baily S A, Zhou H, Ugurlu O, Kennison J A, Dowden P C, Holesinger T G, Foltyn S R and Civale L 2009 *Nat. Mater.* **8** 398

[38] Basov D N, Puchkov A V, Hughes R A, Strach T, Preston J, Timusk T, Bonn D A, Liang R and Hardy W N 1994 *Phys. Rev.* B **49** 12165

[39] Blatter G, Feigelman M V, Geshkenbein V G, Larkin A I and Vinokur V M 1994 *Rev. Mod. Phys.* **66** 1125

[40] Thompson J R, Sun Y R, Christen D K, Civale L, Marwick A D and Holtzberg F 1994 *Phys. Rev.* B **49** 13287(R)

[41] Maley M P, Willis J O, Lessure H and McHenry M E 1990 *Phys. Rev.* B **42** 2639

[42] Ossandon J G, Thompson J R, Christen D K, Sales B C, Yangren S and Lay K W 1992 *Phys. Rev.* B **46** 3050

[43] Haberkorn N, Jeehoon K, Suárez S, Jae-Hun L and Moon S H 2015 *Supercond. Sci. Technol.* **28** 125007

[44] Eley S, Leroux M, Rupich M W, Miller J D, Sheng H, Niraula P M, Kayani A, Welp U, Kwok W K and Civale L 2017 *Supercond. Sci. Technol.* **30** 015010

[45] Thompson J R, Krusin-Elbaum L, Civale L, Blatter G and Field C 1997 *Phys. Rev. Lett.* **78** 3181

[46] Altarawneh M M, Collar K, Mielke C H, Ni N, Bud'ko S L and Canfield P C 2008 *Phys. Rev.* B **78** 220505(R)

[47] Yuan H Q, Singleton J, Balakirev F F, Baily S A, Chen G F, Luo J L and Wang N L 2009 *Nature* **457** 565

[48] Kano M, Kohama Y, Graf D, Balakirev F, Sefat A S, McGuire M A, Sales B C, Mandrus D and Tozer S W 2009 *J. Phys. Soc. Japan* **78** 084719